Postharvest Biology and Technology 205 (2023) 112501

Contents lists available at ScienceDirect

Postharvest Biology and Technology

journal homepage: www.elsevier.com/locate/postharvbio

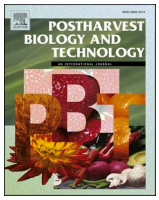

Tissue-specific modulation of functional stress responsive proteins and organic osmolytes by a single or dual short-term high CO_2 treatment during long-term cold storage Autumn Royal table grapes

María Vazquez-Hernandez, Irene Romero, María Teresa Sanchez-Ballesta, Carmen Merodio, María Isabel Escribano *

Grupo Biotecnología y Calidad Posrecolección, Departamento de Caracterización, Calidad y Seguridad, Instituto de Ciencia y Tecnología de Alimentos y Nutrición, ICTAN-CSIC, José Antonio Novais 6, Ciudad Universitaria, E-28040 Madrid, Spain

ARTICLE INFO

Keywords:
Dehydrin isoforms
Organic osmolytes
Pericarp microstructure
Thaumatin-like proteins
Subcellular localization
Vitis vinifera

ABSTRACT

Plant cell response to damage from environmental stressors that cause dehydration involves stress-related proteins and osmotically active compounds whose constitutive levels increase in association with the tolerance response mechanism. In table grape postharvest scope, the application of a second 3 d 20 kPa CO_2 treatment significantly reduced the incidence and severity of long-term cold postharvest storage disorders in Autumn Royal cv. counteracting ultrastructural cell damage and restraining intracellular and membrane oxidative stress. In this sense, it may be of relevance to postharvest quality to know how this dual short-term high CO_2 treatment modulates the cell stress responsive defense strategies, and whether these are tissue-dependent and timing-regulated. In this work, we studied the differential profile of protective osmolytes proline, glycine betaine, γ-aminobutyric acid and trehalose in the berry tissues. Likewise, we assessed the temporal and spatial expression and accumulation patterns of the thaumatin-like protein (VviTL1, VviOsmo) and dehydrin (VviDHN1a, VviDHN4, VviDHN2, VviDHN2D) isoforms in the whole berry tissues and rachis of cv. Autumn Royal table grapes during long-term cold storage period and evaluated the profile-shift by CO_2 treatments. Their subcellular localization in the pericarp tissues was also determined by immunocytochemical transmission electron microscopy (TEM). The results showed that the cold-drought defense strategies activated by the short-term high CO_2 are dose-dependent, tissue-specific and transcriptionally timing-regulated during long-term postharvest cold storage period in table grapes. The results also showed that the more short-term high CO_2 treatment is applied to Autumn Royal grapes, the more microstructural evidence there is of enhanced tolerance to storage disorders in terms of thicker and denser cell wall that could contribute to restrain swelling, dehydration and osmotic stress.

1. Introduction

Biological stress, which includes biotic and environmental stresses, such as drought, high salinity and low temperature, can be a major cause of pre- and postharvest losses. In addition, one biological stress can induce secondary stresses, such as osmotic and oxidative stress, metabolic dysfunction and damage to cellular components (Sharma et al., 2012). Postharvest senescence-related disorders are ultimately associated with the breakdown of cell structures and with important changes in cell wall composition, leading to water loss, fruit softening and increased susceptibility to fungal attack (Tian et al., 2013). Consequently, physiological water loss and oxidative damage are among the many postharvest disorders in the fresh fruit industry that postharvest technologies must control to maintain optimal fruit quality for longer.

Plants have developed systematic defense mechanisms to cope with various biological stresses. The cellular response involves the redirection of metabolism towards the synthesis of several low molecular weight organic molecules, including sugars, sugar alcohols, free amino acids and quaternary amines, which act as osmoprotectants. Nonetheless, in low accumulation, directly protect macromolecules either by stabilizing membranes and the tertiary structure of proteins or by scavenging reactive oxygen species (Ashraf and Foolad, 2007). Similarly, the gene-expression reprogramming of structurally and functionally cell protective macromolecules, such as hydrophilic proteins like dehydrins

* Corresponding author.
E-mail address: escribano@ictan.csic.es (M.I. Escribano).

https://doi.org/10.1016/j.postharvbio.2023.112501
Received 18 April 2023; Received in revised form 13 July 2023; Accepted 27 July 2023
Available online 1 August 2023

and osmotolerance proteins like osmotins, are associated with the maintenance of cellular water and antioxidant status, preventing dehydration disorders (Kosová et al., 2011).

Dehydrins, a subgroup of late embryogenesis abundant (LEA) proteins, are a multifunctional family of hydrophilic and intrinsically disordered proteins that play various protective roles in plants against low temperature and dehydration induced damage (Yu et al., 2018). Accumulation of dehydrin transcripts or proteins has been reported to be associated with increased plant tolerance to environmental stresses that cause cellular water loss (Bao et al., 2017). Recent studies have shown that most of the dehydrins studied have an additional function beyond the classical role of molecular chaperones, acting as radical scavengers, protecting *in vitro* freeze-labile enzymes, acting as cryoprotectors, preventing ice-crystal growth in a manner similar to antifreeze proteins, and participating in the maintenance of the original cell volume and the distance between complexes, thus preventing cell collapse, which allows them to interact peripherally with membranes to favor their stability (Yu et al., 2018; Vazquez-Hernandez et al., 2021).

Thaumatin-like proteins (TLPs) comprise a large multigenic family, classified as members of family 5 of pathogenesis-related proteins (PRs) on the basis of their sequences, serological relationship and biological activities. TLPs include proteins such as thaumatins, osmotins and zeamatins that are involved in systematically acquired resistance and stress response in plants. Although the defensive role of this protein family has been the focus of most research it has also been shown to have other biological functions. Thaumatin-like proteins are induced in response to cold and they have been shown to have antifreeze or cryoprotective properties *in vitro*, and may therefore be functionally involved in the maintenance of macromolecular and membrane stability, playing an active role in cold and freezing dehydration tolerance (Newton and Duman, 2000; Griffith and Yaish, 2004). Furthermore, overexpression of these genes in transgenic plants is known to confer tolerance to various abiotic stresses, including cold, salt and drought (Liu et al., 2010). In this sense, constitutive overexpression of osmotin in tomato modulates the expression of other stress-responsive genes involved in various stress-alleviation functions such as osmotic adjustment and antioxidant defense (Patade et al., 2013).

Low temperature storage combined with high relative humidity is one of the most widely used postharvest technologies to extend fruit commercial quality, as it slows down the rate of metabolism and senescence related events (Sevillano et al., 2009). However, although table grapes are cold tolerant fruit low temperatures can cause structural damage and metabolic and physiological dysfunction which could increase their susceptibility to decay and water loss, increasing the rate of berry abscission and softening, as well as rachis browning (Rosales et al., 2013; Vazquez-Hernandez et al., 2018; Vazquez-Hernandez et al., 2020). Pretreatment with high CO_2 levels (20 kPa CO_2 + 20 kPa O_2 + 60 kPa N_2) for three days is an effective coadjuvant technique for low temperature storage technology to counteract ion and water loss, oxidative membrane damage and decay incidence during postharvest cold storage and shelf life period of Cardinal cv. table grapes without affecting the intrinsic quality of the product (Blanch et al., 2014; Vazquez-Hernandez al., 2018). In terms of cellular water stress, we recently established that different dehydrin isoforms and trehalose may be involved in the cold tolerance mechanism activated by high CO_2 levels in skin tissues of Cardinal table grapes (Navarro et al., 2015). We also reported that the cold-responsive expression levels of thaumatin-like isoforms in Cardinal cv. berries were more related to changes in the cryoprotective activity of skin protein extracts than to the control of fungal decay (Vazquez-Hernandez et al., 2018). Therefore, this PR-5 protein family may play an active role in the cold tolerance of table grape through additional novel activities.

Recently our group showed that the application of a second short-term 20 kPa CO_2 treatment was more effective in prolonging the intrinsic freshness quality than the pretreatment at the beginning of cold storage in controlling clusters dehydration, rachis browning and total decay in the seedless Autumn Royal cv. table grapes stored at 0 ºC for up to 41 d (Vazquez-Hernandez et al., 2020). At the microstructural and metabolic levels, short-term CO_2 treatments reduced the severity of long-term cold storage disorders by counteracting ultrastructural cell damage and restraining intracellular cell and membrane oxidative stress and lipid peroxidation by increasing 18-carbon fatty acid unsaturation, lipid unsaturation ratio, and unsaturated fatty acid index in membrane polar lipids (Vazquez-Hernandez et al., 2020). Furthermore, in line with previous studies that reported a marked difference in the transcriptome profiling of berry tissues (Becatti et al., 2010), the analysis of the composition of the polar lipid fraction shows that the induced-CO_2 cold-tolerant molecular responses are tissue-dependent.

In order to contribute to the understanding of the physiological and molecular mechanisms underlying the differences in the cell susceptibility to cold-oxidative and ultrastructural damage in CO_2-treated table grapes during postharvest cold storage, the present work focuses on 1) the microstructural modification of pericarp cells, 2) the differential profile of protective osmolytes such as proline, glycine betaine, γ-aminobutyric acid (GABA) and trehalose in berry tissues, and 3) the temporal and spatial expression of thaumatin-like proteins and dehydrins in the whole berry tissues and rachis of cv. Autumn Royal table grape clusters during long-term cold storage period and after single or dual short-term 20 kPa CO_2 treatment. The biological protective role of these multifunctional organic osmolytes and stress-responsive protein families is discussed in relation to their tissue and cellular localization, protective metabolite profile and the differences in the timing and extent of transcript expression and accumulation of the different isoforms during cold-storage and after high CO_2 treatments.

2. Material and methods

2.1. Plant material and postharvest treatments

Seedless table grapes (*Vitis vinifera* L. cv. Autumn Royal) were harvested at mature stage (12.9% total soluble solids, 0.46% tartaric acid) from a commercial farm in Abarán (Murcia, Spain). Handling and short 20 kPa CO_2 treatments were performed as described in Vázquez-Hernández et al. (2020). Briefly, grapes were divided into three lots thatś were stored in the dark at 0 ± 0.5 ºC and 90–95% relative humidity: one lot was stored in air (untreated), a second lot was treated with 20 kPa CO_2 + 20 kPa O_2 + 60 kPa N_2 gas mixture for 3 d at the beginning of the cold storage (CO_2-treated), and a third lot was re-exposed to a 3 d 20 kPa CO_2 + 20 kPa O_2 + 60 kPa N_2 treatment after 13 d of storage at 0 ºC (CO_2/CO_2-treated). After the single or dual short-term high CO_2 treatment, bunches were transferred to air until day 41 of storage at 0 ºC. Skin, pulp and primary rachis were collected periodically.

2.2. Microstructural analyses of pericarp cells

Light microscopy was used to examine the microstructure of the pericarp tissues (exocarp and outer mesocarp) of the berries. Six freshly harvested berries were cut transversely into 1 mm thick discs and rectangular pieces (3 mm width × 5 mm length) were collected, fixed, dehydrated embedded in Spurŕs resin (Dow Chemical Co., USA) and polymerized according to the method described by Vazquez-Hernandez et al. (2020). For microstructural observations, transverse semithin Section (2 μm thick) of polymerized samples were cut using a microtome (Leica RM2016, Germany) and stained on microscopic slides, containing a 10% acetone in distilled water and heated to 122 ºC to evaporate the acetone. After washing with 1% periodic acid in distilled water for 5 min and twice with distilled water, the sections were stained with 1% toluidine blue O (TBO) in 1% sodium tetraborate solution for 5 min at 60 °C. The samples were examined by Light Transmission Microscopy using a Zeiss Axioplan-2 Microscope (Oberkochen, Germany). Four sections were cut from each biological sample and several cells in each section

were analyzed (ICTS National Center of Cytometry and Fluorescence Microscopy facility, University Complutense, Madrid, Spain). The micrographs shown are representative of the results obtained from six biological samples.

2.3. Immunogold electron microscopy

The subcellular distribution of thaumatin-like proteins and dehydrins was analyzed in the pericarp of berries (exocarp and outer mesocarp cells) by immunogold labelling transmission electron microscopy (TEM). Six freshly harvested berries were cut transversely into 1 mm thick discs and rectangular pieces (3 mm width × 5 mm length) were immediately fixed for 2 h at 4 ºC in PBS pH 7.2 with 1% (v/v) glutaraldehyde and 4% (v/v) paraformaldehyde. After intensive washing with PBS, the tissues were dehydrated in a graded ethanol series, 30–100% (v/v) for 30 min each time, and embedded in LR-White resin (London resin Company, London, UK) overnight and polymerized at 60 ºC for 48 h according to Chen et al. (2006). Ultrathin sections (60–70 nm) were cut with a diamond knife on an ULTRACUT E ultramicrotome (Reichert-Jung, Austria) and collected on 100-mesh Formvar-coated nickel grids. Grids containing ultrathin sections were sequentially floated in 0.1 M glycine in PBS and 5% BSA in PBS. Grids were incubated overnight at 4 ºC with rabbit anti-PR-5 or anti-dehydrin diluted 1:75 in PBS containing 1% BSA, washed with PBS and incubated for 1 h at room temperature with the secondary antibody, goat anti-rabbit IgG conjugated to 10-nm gold particles (British Biocell, Cardiff, UK) diluted 1:100 in PBS. After PBS and water washes, sections were stained with 2% aqueous uranyl acetate for 20 min and Reynolds' lead citrate for 3 min and examined using a JEOL JEM 1010 Transmission Electron Microscope (Tokio, Japan) at an acceleration voltage of 100 kV. Controls were included by excluding the primary antibody. Four sections were cut from each biological sample and several cells in each section were analyzed (ICTS National Center of Electron Microscopy facility, Complutense University, Madrid, Spain). The micrographs shown are representative of the results obtained from six biological samples.

2.4. Protein extraction and immunodetection

Extraction of the total protein fraction from skin, pulp and rachis tissues and immunodetection of thaumatin-like and dehydrin isoforms were performed as previously described by Vazquez-Hernandez et al. (2018). Briefly, proteins were separated by SDS-PAGE (13.5–15% polyacrylamide) and electro-transferred to PVDF membranes (Amersham). The membranes were probed with a polyclonal anti-dehydrin antiserum (1/10000: Agrisera) and with tobacco anti-PR-5 (1/12000) antisera, which were detected with a horseradish peroxidase conjugated rabbit antiserum against IgG (Amersham). Immuno-complexes were visualized using a chemiluminescence (ECL®) detection system (Amersham) and ChemiDoc™ XRS gels analysis and documentation equipment with ImageLab software ™ (Bio-Rad). Independent experiments were performed in at least triplicate.

2.5. Mass spectrometry analysis

For VviOsmo protein identification, frozen skin tissue was homogenized in 0.1 M sodium acetate buffer, pH 5.0, heated at 95 ºC for 15 min, cooled on ice for 10 min and centrifuged to remove debris and coagulated proteins. The acid-soluble and heat-stable protein fraction was mixed with an equal volume of 2x Laemmli sample buffer containing 2.5% β-mercaptoethanol and heated at 95 ºC for 5 min. Proteins with a M_r range between 20 and 100 kDa were separated by SDS-PAGE (13.5% polyacrylamide). The 23 like-thaumatin band was excised from the corresponding Coomassie-stained gel and aligned with the corresponding Western blot, using pre-stained molecular mass standard proteins to identify the region of interest. The Coomassie bands were subjected to tryptic digestion and analyzed by MALDI-MS for peptide mass fingerprint (PMF) identification, followed by post-source decay MS/MS analysis on a MALDI-TOF/TOF 4800 Plus Proteomics Analyzer (Applied Biosystems) in positive ion delayed extraction reflector mode according to the procedure described in Goñi et al. (2010).

Spectra were analyzed using the 4000 Series Explorer v 3.0 software (Applied Biosystems) and the Matrix Science MASCOT search engine (www.matrixscience.com) against the non-redundant NCBI database (http://www.ncbi.nlm.nih.gov; NCBInr). The database was searched using PMF and internal peptide sequence analysis by MS/MS. The instrument type specified for the MS/MS ion searches was MALDI-TOF-TOF and the search parameters were set according to Goñi et al. (2010). The peptide fragments generated above were subjected to the automated *de novo* sequencing using DeNovo Explorer software (Applied Biosystems) and a homology search was performed against the NCBInr database (Proteomic Facility UCM-PCM, Madrid, Spain).

2.6. Relative gene expression by semi-quantitative and quantitative RT-PCR

Total RNA extraction and cDNA synthesis were performed according to Romero et al. (2016). The relative expression of *VviTL1*, *VviOsmo* and *VviDHN4* spliced and unspliced transcripts in the skin, pulp and rachis of CO_2-treated, CO_2/CO_2-treated and untreated clusters stored at 0 ºC was determined by RT-qPCR as described by Rosales et al. (2013), using gene-specific primer pairs (Vazquez-Hernandez et al., 2017; Romero et al., 2021). *Actin1* (XM_002282480) from *V. vinifera* was used as internal control. The specificity of the products was validated by dissociation curve analysis and by agarose gel; and their sequences were confirmed by Sanger sequencing at the Genomics Department of the CIB-CSIC (Madrid, Spain). Each gene was evaluated in at least two independent runs. The relative expression levels in three biological samples were estimated by the $2^{-\Delta\Delta Ct}$ method and expressed as the fold difference from the expression present in the prestored fruit.

Spliced and unspliced variants of *VviDHN1a* and *VviDHN2* were assessed by semiquantitative RT-PCR as described by Navarro et al. (2015), using specific primer pairs (Vazquez-Hernandez et al., 2017) and *Actin1* as an internal control. After amplification, products were visualized by electrophoresis on a 2% agarose gel stained with Goldview (Guangzhou Geneshun Biotech Ltd.). The identification of each PCR product was confirmed by Sanger sequencing at the Genomics Department of the CIB-CSIC (Madrid, Spain). Experiments were performed independently in at least triplicate.

2.7. Chromatographic determination of organic osmolytes

Determination of GABA, proline and glycine betaine levels in skin and pulp tissues was performed according to the method described by Vazquez-Hernandez et al. (2018) using Q-TOF LC-MS equipped with a Zorbax Eclipse XDB-C8 5 μm, 4.6 × 150 mm column (Agilent Technologies) and eluted with an isocratic mobile phase consisting of a mixture (75:25) of deionized water containing 0.1% heptafluorobutyric acid and 0.1% formic acid (solvent A), and acetonitrile (solvent B), at a flow rate of 1 mL min^{-1} at 30 ºC. GABA, proline and glycine betaine were identified by their retention time and *m/z* data and quantified using a calibration curve derived from standards (Analysis Service Unit facilities, ICTAN, Madrid, Spain). Amino acid content was expressed as μmol per kg of fresh weight. The mean data of two analyses on three different biological samples are presented.

The determination of trehalose content in skin and pulp tissues was performed as described by Navarro et al. (2015) using high-performance anion-exchange chromatography with pulsed amperometric detection (HPAEC-PAD), equipped with a Hamilton RCX30 column (250 × 4.6 mm, 5 μm particle size) and eluted with an isocratic gradient of 150 mM NaOH over 10 min at a flow rate of 1 mL min^{-1} (Analysis Service Unit facilities, ICTAN, Madrid, Spain). Trehalose content was expressed as μmol per kg of fresh weight. The mean data of two analyses on three

different biological samples are presented.

2.8. Statistical analysis

One-way ANOVA was performed using SPSS Statistics ver. 27.0. (IBM Corporation). Multiple comparisons of means were performed using the Tukey's test, with a significance level of $P \leq 0.05$.

3. Results

3.1. Effect of short-term high CO_2 treatments on cell microstructure in Autumn Royal table grape berry tissues after prolonged cold storage

The morphology of the pericarp of Autumn Royal table grapes was studied by optical microscopy at different magnifications (10x and 100x) on transverse sections stained with toluidine blue O (Fig. 1). In the 10x images, the mesocarp tissues (pulp) and the exocarp tissues (skin) can be distinguished by their cell size and shape. The mesocarp contained uncolored, turgid, voluminous and thin-walled parenchymatous cells. In the exocarp tissues, three layers can be differentiated: the cuticle, covered by epicuticular waxes; the underlying epidermis which appears as a regular tiling of cells with moderately thick walls and is separated from the mesocarp by the third layer; the hypodermis, composed of a variable number of collenchymatous layers, containing uncolored cells, colored cells (with phenolic compounds) and cells containing black spherical inclusions of a lipid nature (plastoglobules) (Fig. 1).

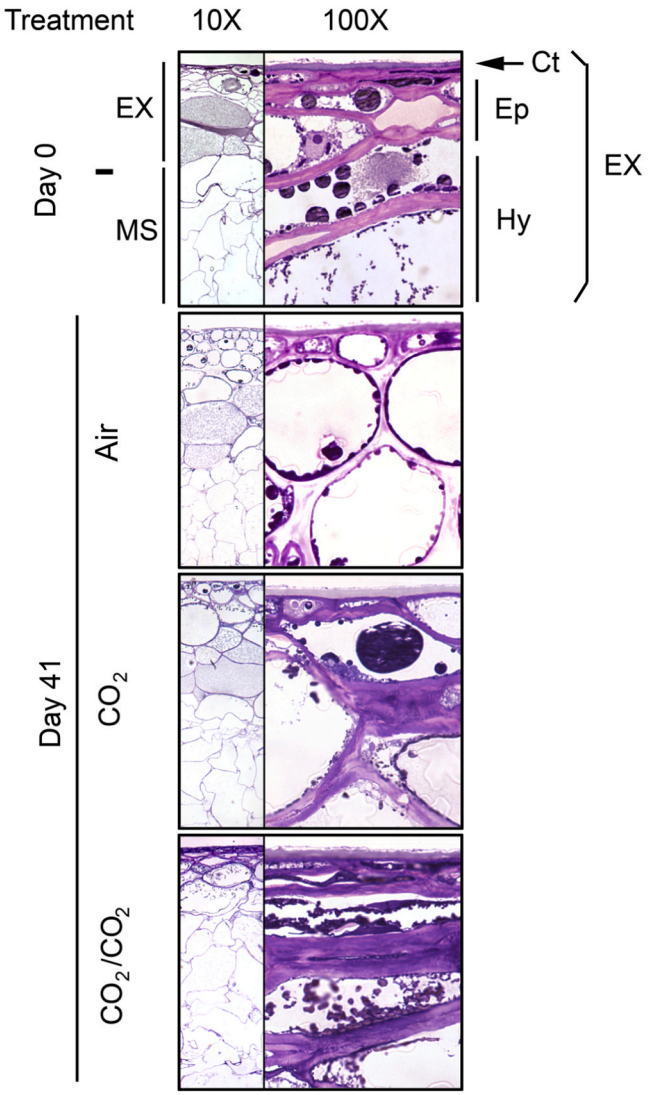

Fig. 1. Cellular pericarp microstructure of prestored (day 0), untreated (Air), CO_2-treated (CO_2) and CO_2/CO_2-treated (CO_2/CO_2) Autumn Royal table grapes after storage for 41 d at 0 °C. Observations of pericarp micrographs obtained by light microscopy stained with toluidine blue-O. Ex: exocarp; Ms: mesocarp; Ct: cuticle; Ep: epidermal cell layers; Hy: hypodermal cell layers. Scale bars: 10x and 100x. The micrographs shown are representative of six biological samples.

In general, no cell microstructural changes were observed in mesocarp tissues due to prolonged cold storage or treatments apply. On the contrary, the exocarp layers of grapes show histological changes due to cold storage and/or CO_2 treatment, which are better observed in 100x images. Under the cuticle, freshly harvested fruit epidermis and outer-hypodermis showed thick-walled flattened cells, with high affinity for toluidine blue O, and with small intercellular spaces. After 41 d of cold storage, the walls gradually lost their staining intensity and became thin-walled, giving the cells a rounded appearance (swollen cells) with large intercellular spaces, causing the delimitation between the epidermis and the outermost layers of the hypodermis to become more diffuse (Fig. 1). At the end of long-term cold-storage, CO_2-treated table grapes showed an epidermis of similar thickness to that of the prestored fruit, with more flattened shape, dye-good affinity and thick-walled cells. A second short-term 20 kPa CO_2 treatment resulted in the formation of an even more compact epidermis, with cell walls that widened and appeared even thicker, intensifying their pink-purple color, and with cells that reduced their intracellular and intercellular spaces (Fig. 1).

3.2. Effect of high CO_2 treatments on organic protective osmolytes in Autumn Royal table grape berry tissues during cold storage

The levels of low molecular weight osmoprotective solutes, such as trehalose, proline, glycine betaine and GABA, were quantified in the skin and pulp tissues of prestored Autumn Royal table grapes and during low temperature storage at 0 °C, with and without 20 kPa 3-d CO_2 treatments. The results showed that, despite the different initial endogenous trehalose levels, 85 ± 7.5 in skin and 10 ± 0.6 μmol per kg of fresh weight in pulp tissues, low temperature induced a moderate increase in the endogenous levels in skin tissues, which was maintained throughout the long-storage period. One and particularly two-time short-term CO_2 treatments significantly ($P \leq 0.05$) increased trehalose levels during cold storage compared to those in the skin of untreated (Air) berries (Table 1).

Quantification of the endogenous levels of proline, glycine betaine and GABA by Q-TOF LC-MS showed that, in contrast to trehalose, the pulp tissues of prestored berries contained higher levels of nitrogenous osmolites than the skin tissues, in the order of 4.8-times of proline (2150 ± 30 *versus* 450 ± 9 μmol per kg of fresh weight), 2.5 times of glycine betaine (40 ± 1.7 *versus* 16 ± 0.4 μmol per kg fresh weight) and 2.0 times of GABA (110 ± 4 *versus* 55 ± 2 μmol per kg fresh weight). Overall, while 3 d of cold storage significantly ($P \leq 0.05$) increased the endogenous levels of the nitrogenous compounds, the length of cold exposure and the environmental storage conditions modified the profile of these organic osmolytes in a tissue-dependent manner. It should be noted that the levels of the nitrogenous organic osmolytes decreased at the end of cold storage in both tissues. On the other hand, 3-d CO_2 treatments raised proline levels in berries, especially when a second short-term high CO_2 was applied after 13-d of cold storage. Afterwards, whereas a slight decrease in proline levels was achieved in skin tissues of treated berries, a progressive increased was observed in the pulp tissues. At the end of the storage period, the pulp tissues of treated berries reached 3-fold higher relative proline levels than in CO_2 and CO_2/CO_2-treated skin tissues, and up to more than 4-fold and 6-fold higher levels than those achieved in untreated (Air) pulp tissues in one- and two-time CO_2 treated fruit, respectively (Table 1). With regard to glycine betaine, despite the differences in tissue levels in prestored fruit, a similar and moderate increase was shown in both CO_2 and CO_2/CO_2 treated berry

Table 1
Organic osmolytes levels, expressed as μmol kg^{-1} fresh weight, in the skin and pulp of prestored and in untreated (Air) and treated with 20 kPa CO_2 (CO_2-treated; CO_2/CO_2-treated) Autumn Royal table grapes during storage at 0 ºC.

	Skin				Pulp			
Days at 0 ºC	Trehalose	Proline	Glycine betaine	GABA	Trehalose	Proline	Glycine betaine	GABA
Prestored								
0 d	85a	450a	16a	55a	10a	2150a	40a	110a
Air								
3 d	105 (20)b	492 (42)b	30 (14)c	96 (41)b	13 (3)ab	2250 (100)b	48 (8)b	183 (73)b
16 d	115 (30)c	500 (50)b	28 (12)c	123 (68)b	15 (5)b	2270 (120)b	50 (10)b	145 (35)ab
28 d	110 (25)b	510 (60)b	25 (9)b	176 (121)c	16 (6)b	2280 (130)b	52 (12)b	197 (87)b
41 d	115 (30)c	470 (20)a	23 (7)b	145 (90)b	12 (2)a	2205 (55)a	53 (13)b	181 (71)b
CO_2-treated								
3 d	139 (54)d	565 (115)d	40 (24)e	225 (170)d	18 (8)b	2330 (180)c	57 (17)c	256 (146)c
16 d	135 (50)d	555 (105)d	30 (14)c	180 (125)c	17 (7)b	2320 (170)c	55 (15)bc	216 (106)b
28 d	124 (39)c	540 (90)d	26 (10)b	201 (146)c	19 (9)c	2366 (216)c	59 (19)c	259 (149)c
41 d	135 (50)d	525 (75)c	29 (13)c	264 (209)d	18 (8)b	2382 (232)d	59 (19)c	264 (154)c
CO_2/CO_2-treated								
16 d	145 (60)e	590 (140)e	33 (17)c	230 (175)d	21 (11)c	2412 (262)d	60 (20)c	266 (156)c
28 d	137 (52)d	620 (170)e	28 (12)c	217 (162)d	22 (12)c	2431 (281)d	64 (24)d	238 (128)bc
41 d	145 (60)e	566 (116)d	32 (16)c	325 (270)e	20 (10)c	2495 (345)f	62 (22)cd	322 (212)d

Data represent the mean of three biological replicates (n = 6) and each letter within columns indicates the significant differences between means determined with a Tukey's test ($P \leq 0.05$). Data in parenthesis express the relative change with respect to the levels in prestored fruit (day 0).

tissues, maintaining higher endogenous levels of the quaternary ammonium in the pulp throughout the 41 d at 0 ºC in all postharvest storage conditions (Table 1). In relation to the organic osmolyte GABA, its metabolism responds differently to cold and high levels of CO_2 in each tissue. Although in pulp tissues of treated berries the levels of this non-protein amino acid increased in a CO_2 dose-dependent manner, it is in skin tissues that a higher relative accumulation of GABA was achieved due to the effect of CO_2 treatments, reaching similar levels to those in the pulp tissues at the end of the 41 d of cold storage, despite the lower titers present in the skin of prestored fruit. The relative increase levels in the skin tissues of berries treated once and twice with CO_2 were up to 4- and 5-fold higher than those of prestored berries and 2- and 3-fold higher than those of untreated berries (Table 1).

3.3. Effect of high CO_2 treatments on the protein accumulation and gene expression patterns of thaumatin-like isoforms in Autumn Royal table grape berry tissues and rachis during cold storage

After harvest, two polypeptides with an apparent molecular mass of 23 kDa and 24 kDa are recognized by the tobacco PR-5 (thaumatin-like proteins) antisera in Autumn Royal table grapes. These proteins are differentially expressed in berry tissues (skin and pulp) and rachis (Fig. 2A). While both polypeptides were constitutively detected in skin and pulp tissues, albeit at different levels, only the low molecular mass thaumatin-like isoform was detected in rachis. In *V. vinifera*, the two most expressed thaumatin-like genes encode a thaumatin (*VVLT1*) and an osmotin (*VVOSM1 / VVLT2*) protein. These proteins have a similar molecular mass of around 24 kDa. In order to establish the identity of the more abundant recognized thaumatin-like polypeptides in the berry tissues and rachis (Fig. 2A), the isolated Coomassie-stained band corresponding to the 23 kDa protein isoform was subjected to tryptic digestion and analyzed by MALDI-TOF MS coupled to tandem mass spectrometry. The NCBInr database search, based on the tryptic peptide mass fingerprint (PMF) obtained and the MS/MS spectra of one of the peptide ion, revealed that 6 peptide fragments (Table 2) of the 23 kDa polypeptide matched significantly (MASCOT protein score > 75, $P < 0.05$) with a 31% sequence coverage with osmotin-like proteins [*V. vinifera*] as AAQ10092 (GI:33329390; 115 score), CAA71883 (GI:1839046; 105 score) and XP_002282988 (GI:225426795; 105 score). Taking this into account, we designed the 23 kDa protein as VviOsmo (osmotin) and the 24 kDa protein as VviTL1 (thaumatin).

To analyze the effect of the postharvest application of short-term treatments with high CO_2 levels on the expression pattern of the thaumatin-like isoforms in Autumn Royal table grapes, VviTL1 and VviOsmo were immunodetected with tobacco PR-5 antisera in berry tissues and rachis throughout the cold storage period (Fig. 2A). Whereas in untreated and one and two-time CO_2-treated skin tissues the accumulation level of thaumatin-like isoforms was maintained at a steady state level during the 41 d of cold storage period, in pulp tissues the abundance of VviTL1 and VviOsmo polypeptides was differentially regulated by the effect of the length cold exposure and environmental storage conditions (Fig. 2A). In this sense, while VviTL1 levels increased in both untreated and CO_2-treated pulp tissues, reaching similar levels, a further increase in the accumulation of the 24 kDa thaumatin-like polypeptide takes place in these two-time CO_2-treated berries. However, the VviOsmo isoform was more responsive to high CO_2 levels, despite the low levels in the pulp of prestored berries, and was up-regulated by single and dual short-term high CO_2 treatments (Fig. 2A). The levels of the 23 kDa protein increased at the end of the CO_2-treatments (3 and 16 d) and maintained these high levels when the fruit were transferred to atmospheric conditions and until the end of the long-term storage period. In rachis tissues, where the 24 kDa isoform was not constitutively expressed, the levels of VviOsmo polypeptide were higher in untreated than those CO_2-treated clusters (Fig. 2A).

In order to better understand the regulation of thaumatin-like genes regulation in Autumn Royal table grapes during cold storage and after postharvest treatments with 20 kPa CO_2 for 3 d, we analyzed the transcript levels of *VviLT1* (thaumatin) and *VviOsmo* (osmotin) these defense-related genes in berry tissues and rachis by semiquantitative RT-PCR. The results showed that in skin tissues, the expression of *VviLT1* and *VviOsmo* was down-regulated after harvest and no significant changes were detected during cold storage or due to CO_2 treatments. On the contrary, in pulp tissues, *VviLT1* and *VviOsmo* are up-regulated after harvest. Whereas in untreated berries, *VviTL1* transcript levels progressively increased and *VviOsmo* maintained a steady state expression level throughout storage period, both genes were transiently up-regulated by a short-term CO_2 treatment at the beginning of storage period (Fig. 2B). Moreover, the application of a second 20 kPa CO_2 treatment for 3 d was able to induce the expression of the *VviOsmo* gene, reaching the highest expression level at the end of the long-term storage period, which was almost 2-fold higher than those of untreated (Air) and one-time CO_2-treated fruit (Fig. 2B). In contrast, in rachis tissues, *VviLT1* and *VviOsmo* transcript levels did not change significantly, with only a slight increase in *VviOsmo* transcripts in untreated samples between 16 and 28 d of the storage and a down-regulation of *VviLT1* and *VviOsmo* due to CO_2 treatments (Fig. 2B).

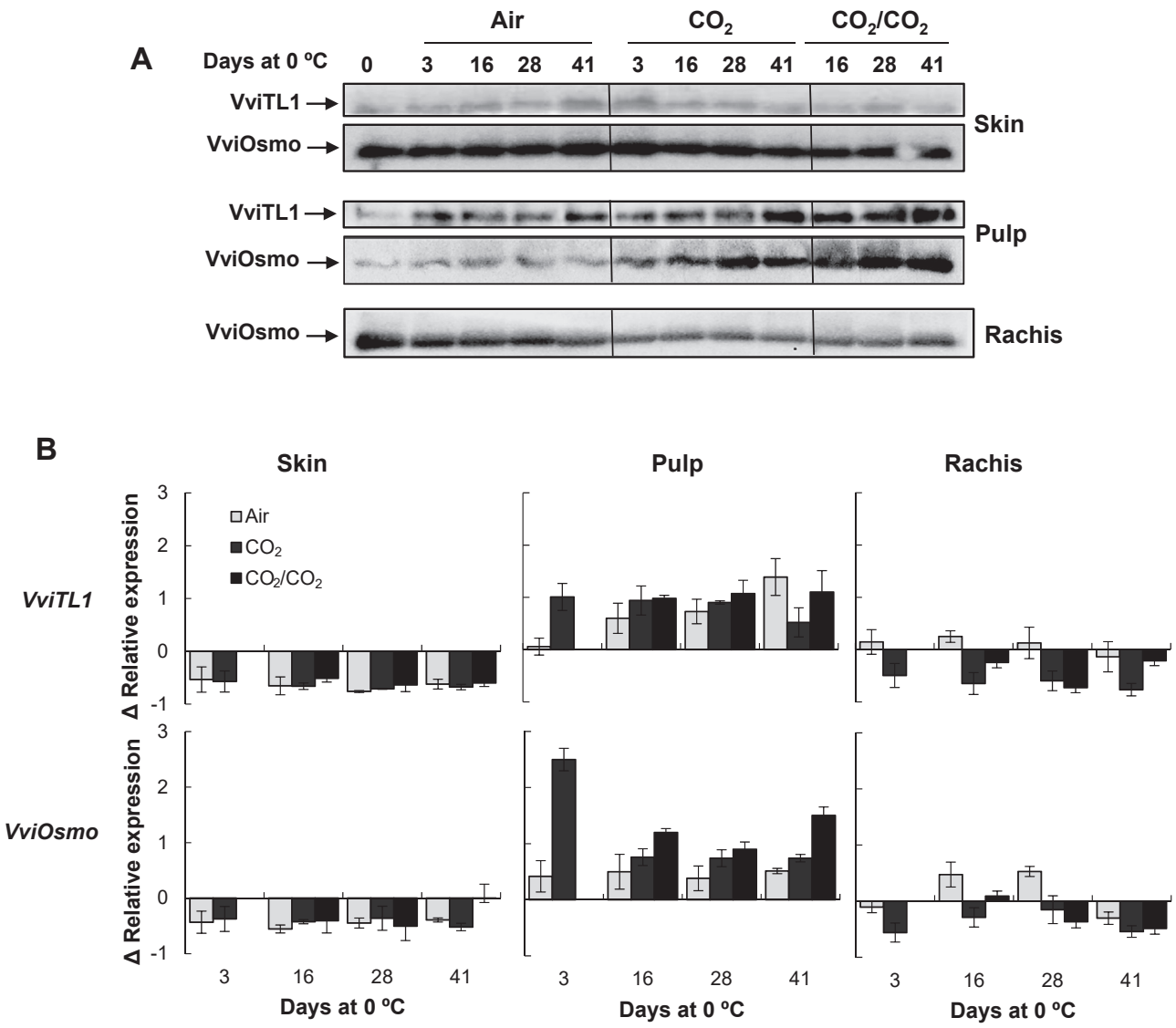

Fig. 2. Immunodetection of thaumatin-like protein isoforms (A) and levels of *VviTL1* and *VviOsmo* (B) in the skin, pulp and rachis of untreated (Air), CO_2-treated (CO_2) and CO_2/CO_2-treated (CO_2/CO_2) Autumn Royal table grapes during storage at 0 ºC. The results shown in A are representative of three biological samples. The relative expression of *VviTL1* and *VviOsmo* transcript levels was estimated using the $2^{-\Delta\Delta Ct}$ method, relative to the calibrator sample (prestored fruit, day 0). Data are mean ± SD of three biological samples.

Table 2
Identification of VviOsmo protein by MS. Amino acid sequences of peptide fragments were obtained by PMF and MS/MS search of the NCBInr database.

Obs. mass[a]	Exp. mass	Calc. mass	Delta	Start seq.	End seq.	Miss	Peptide seq.	MASCOT Ion score
1284.5326	1283.5253	1283.5201	4	72	83	0	R.TNCNFDASGNGK.C	-
1761.8375	1760.8302	1760.8437	-8	143	159	0	R.GISCTADIVGECPAALK.T[b]	83
1455.6281	1454.6208	1454.6283	-5	160	172	0	K.TTGGCNNPCTVFK.T	-
3597.4775	3596.4702	3596.3644	29	160	190	1	K.TTGGCNNPCTVFKTDEYCCNSGSCDATDYSR.F	-
2160.7942	2159.7869	2159.7467	19	173	190	0	K.TDEYCCNSGSCDATDYSR.F	-
1357.6176	1356.6103	1356.6132	-2	194	204	1	K.TRCPDAYSYPK.D	-

[a] Obs., observed; Exp., experimental; Calc., calculated; seq., sequence; Miss, missed cleavage.
[b] Ion peptide sequence confirmed by MS/MS analysis.

3.4. Effect of high CO_2 treatments on the protein accumulation and gene expression patterns of dehydrin isoforms in Autumn Royal table grape berry tissues and rachis during cold storage

A polyclonal antiserum raised against the consensus K-segment (the anti-dehydrin antibody) revealed a tissue-specific dehydrin isoform pattern in prestored table grape clusters (day 0). Whereas the four isoforms VviDHN1a (17 kDa), VviDHN4 (22 kDa), VviDHN2 (27 kDa) and it dimer VviDHN2D (44 kDa) were detected in the skin and rachis, only the two polypeptides with higher molecular mass were immunodetected in the pulp (Figs. 3A, 4A and 5A). The study of the accumulation pattern of tissue-specific dehydrins during postharvest storage revealed that the isoforms differ in their abundance levels and are regulated by environmental factors such as low temperature and high

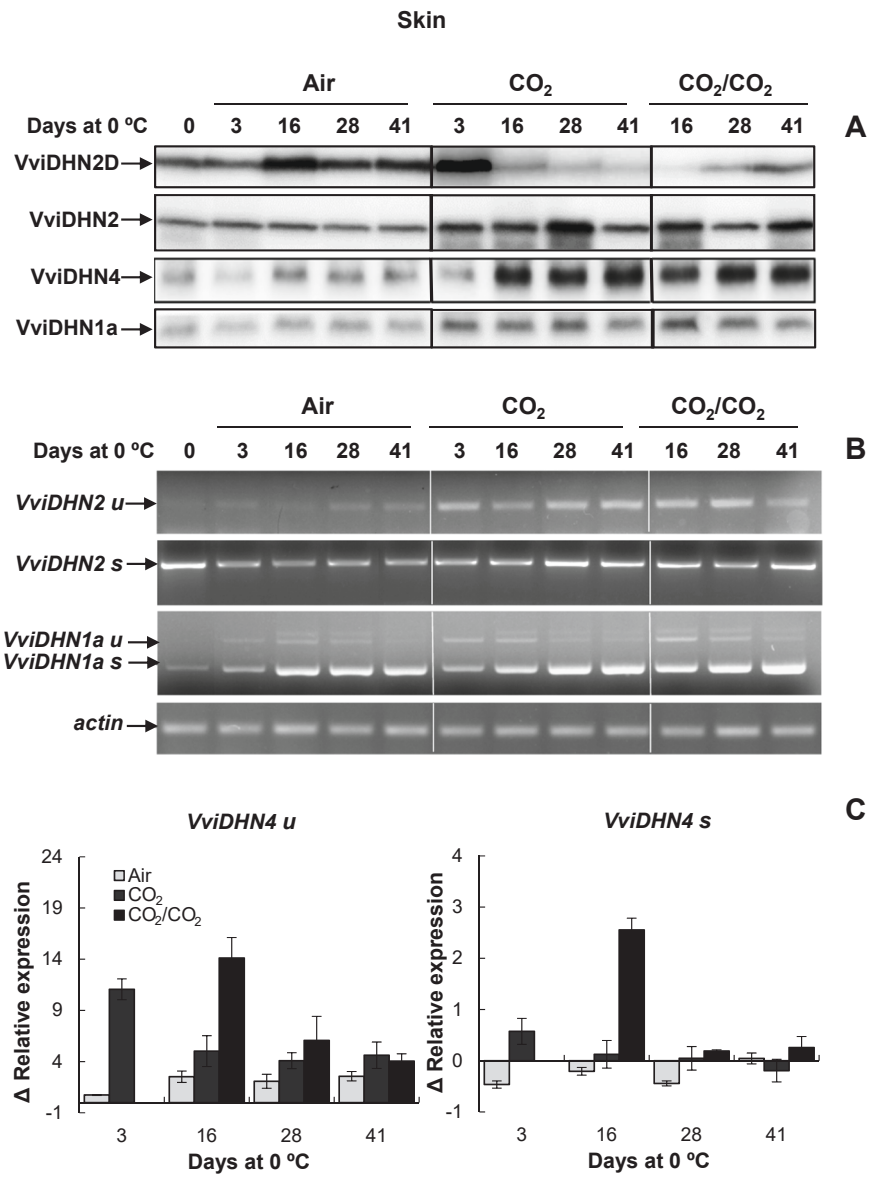

Fig. 3. Immunodetection of dehydrin isoforms (A) and levels of *VviDHN2*, *VviDHN1a* (B) and *VviDHN4* (C) spliced (s) and unspliced (u) mRNAs in the skin of untreated (Air), CO_2-treated (CO_2) and CO_2/CO_2-treated (CO_2/CO_2) Autumn Royal table grapes during storage at 0 ºC. The results shown in A and B are representative of three biological samples. The relative expression of *VviDHN4* spliced and unspliced transcript levels was estimated using the $2^{-\Delta\Delta Ct}$ method, relative to the calibrator sample (prestored fruit, day 0). Data are the mean ± SD of three biological samples.

CO_2.

As shown in Fig. 3A, in berry skin tissue of untreated grapes, while the prestored levels of VviDNH2, VviDHN4 and VviDHN1a did not change during cold storage, a transient increase in VviDHN2D accumulation occurred on the 16th d of storage. Treatment for 3 d with CO_2 at the beginning of cold storage increased the levels of the four dehydrin polypeptides, an effect that was lost in the case of the dimer isoform after table grapes were transferred to air. However, the second short-term CO_2 treatment did not result in an additional increase in dehydrin accumulation (Fig. 3A).

As described above for the dehydrin isoforms, the expression pattern of the spliced and unspliced forms of *VviDHN* gene in different tissues during postharvest storage revealed that they were also differentially regulated by low temperature and high CO_2. In the skin tissues, while low temperature decreased the initial levels of *VviDHN2* and *VviDHN4* spliced forms, a progressive increase in the expression of *VviDHN1as* transcript levels was achieved. However, CO_2 treatments induced the transcription of the three *VviDHN* spliced forms: at the end of one or two-time short-term high CO_2 treatments, as *VviDHN4s*, or throughout the storage period, as *VviDHN2s* and mainly *VviDHN1as* (Fig. 3B and C). Relative gene expression analysis of unspliced forms revealed a transcriptional regulation by CO_2 treatments. While *VviDHN1au* showed a low steady state expression level, *VviDHN2* maintained a higher unspliced transcript abundance in CO_2-treated than in untreated fruit (Fig. 3B), *VviDHN4* is the unspliced form that showed the greatest transcriptional up-regulation by the treatment with 20 kPa CO_2 for 3 d at 0 ºC, mainly at the end (16 d) of the second CO_2 treatment in skin tissues (Fig. 3C).

In the case of the pulp tissues, it should be noted that, in addition to the increase in the intensities of the two highest molecular mass dehydrin isoforms identified in the prestored fruit, the polypeptide bands corresponding to VviDHN4 and VviDHN1a were detected throughout the cold storage (Fig. 4A). CO_2-treatments differentially increased the levels of dehydrin isoforms, mainly VviDHN2D and VviDHN2 in the pulp tissues of one-time CO_2-treated berries, and VviDHN1a in those two-time CO_2-treated (Fig. 4A). It is worth noting that at the end of long-term cold storage, the pulp of treated berries maintained abundant levels of dehydrin isoforms compared to untreated ones, which were more noticeable for VviDHN4 in those two-time short-term CO_2-treated berries (Fig. 4A). In pulp tissues, the *VviDHN2s*, *VviDHN4s* and *VviDHN1as* genes were differentially regulated by cold and CO_2 treatments. In this sense, while *VviDHN4s* maintained a low steady state expression

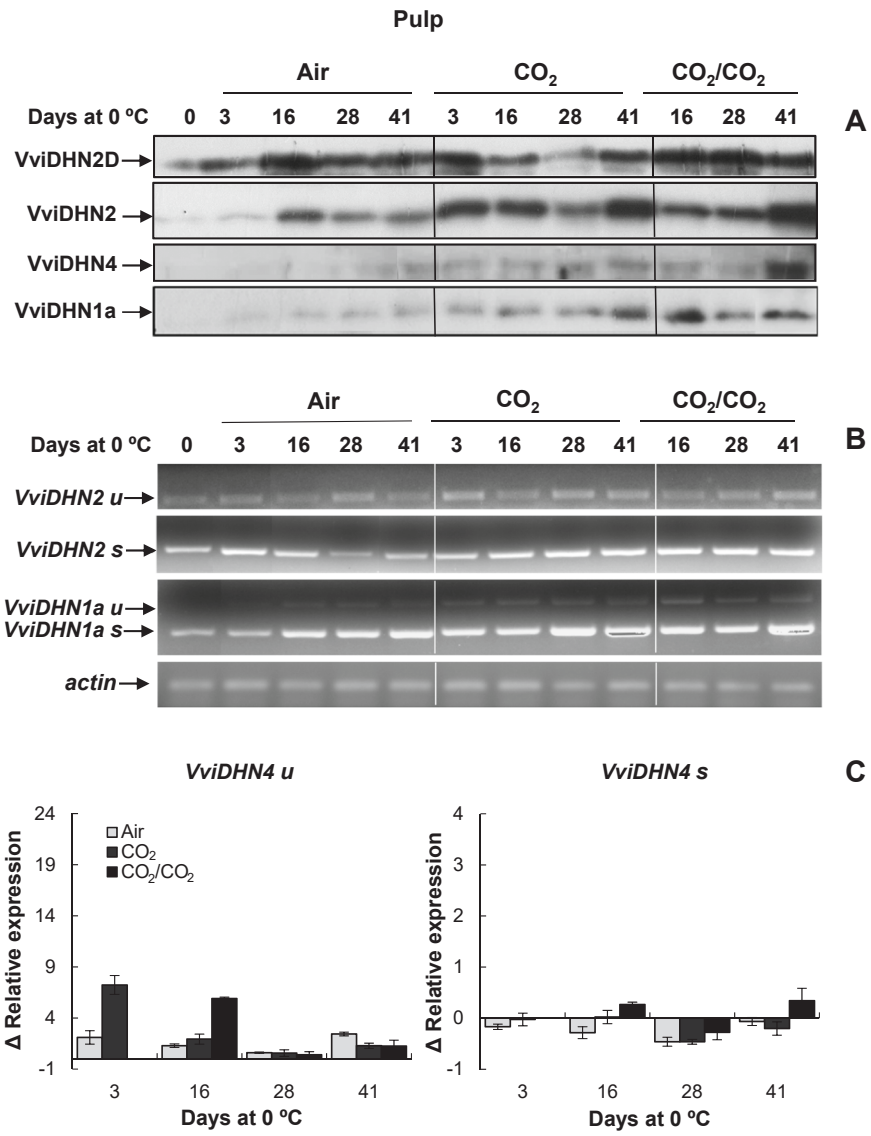

Fig. 4. Immunodetection of dehydrin isoforms (A) and levels of *VviDHN2*, *VviDHN1a* (B) and *VviDHN4* (C) spliced (s) and unspliced (u) mRNAs in the pulp of untreated (Air), CO_2-treated (CO_2) and CO_2/CO_2-treated (CO_2/CO_2) Autumn Royal table grapes during storage at 0 ºC. The results shown in A and B are representative of three biological samples. The relative expression of *VviDHN4* spliced and unspliced transcript levels was estimated using the $2^{-\Delta\Delta Ct}$ method, relative to the calibrator sample (prestored fruit, day 0). Data are the mean ± SD of three biological samples.

level in untreated and CO_2-treated fruit and was transiently induced after 16 and 41 d of storage at 0 ºC in those two-time treated fruit, the spliced *VviDHN2* and *VviDHN1a* forms were up-regulated both by storage at 0 ºC and mainly by exposure to 20 kPa CO_2 treatment (Fig. 4B and C). As described for skin, the unspliced dehydrin forms were differentially CO_2-regulated at the transcriptional level in pulp tissues. While the *VviDHN1as* and *VviDHN2s* forms showed a low steady state expression level, *VviDHN4* maintained a higher abundance of unspliced transcripts in CO_2-treated than in untreated fruit (Fig. 4B and C).

In the rachis, the expression pattern of dehydrin isoforms changes with respect to berry tissues, since a progressive loss of the dehydrin isoforms occurred during cold storage (Fig. 5A). While the treatments with 20 kPa of CO_2 for 3 d increased the levels of VviDHN1a, VviDHN4 and VviDHN2D, and maintained the initial levels of VviDHN2, a gradual decrease was observed afterwards, as well as in the clusters conserved under atmospheric conditions, a progressive decrease was observed, with no expression of dehydrin isoforms detected in the rachis after 41 d of cold storage in any of the atmospheric conditions, except for the dimeric isoform in the CO_2/CO_2-treated table grapes (Fig. 5A). In rachis, whereas the transcription of the *VviDHN2* and *VviDHN4* spliced isoforms was induced by low temperature and high CO_2 at the beginning of storage (3 d) or by long-term cold storage, respectively, the transcription levels of the *VviDHN1a* spliced form maintained a steady state lower induction level throughout the storage period in both untreated and treated table grape bunches (Fig. 5B and C). On the other hand, in rachis, the transcription of *VviDHN2s* and *VviDHN4s* was transiently up-regulated after 3 d of storage at 0 ºC under atmospheric conditions, and by the short-term high CO_2 treatments, which even increased in two-time CO_2 treated rachis (Fig. 5B and C).

3.5. Subcellular localization of thaumatin-like proteins and dehydrins in Autumn Royal table grape berries

The subcellular distribution of thaumatin-like proteins and the spliced form of dehydrins was studied in ultrafine sections of the pericarp (exocarp and outer mesocarp cells) of Autumn Royal table grape using the immunogold electron-microscope technique (Figs. 6 and 7). Note that these patterns cannot be considered representative of the amount of protein in the whole exocarp and mesocarp, as the protein was heterogeneously distributed within the berry skin and pulp, and the images were acquired at high magnification. Furthermore, no gold particles were found, respectively, when the polyclonal antibody against thaumatin-like proteins and dehydrins was omitted during the immunolabeling, suggesting that the immunogold electron-microscopy localizations identified in the experiment were both specific and reliable.

Thaumatin-like proteins were detected in the cell wall (Fig. 6A) as

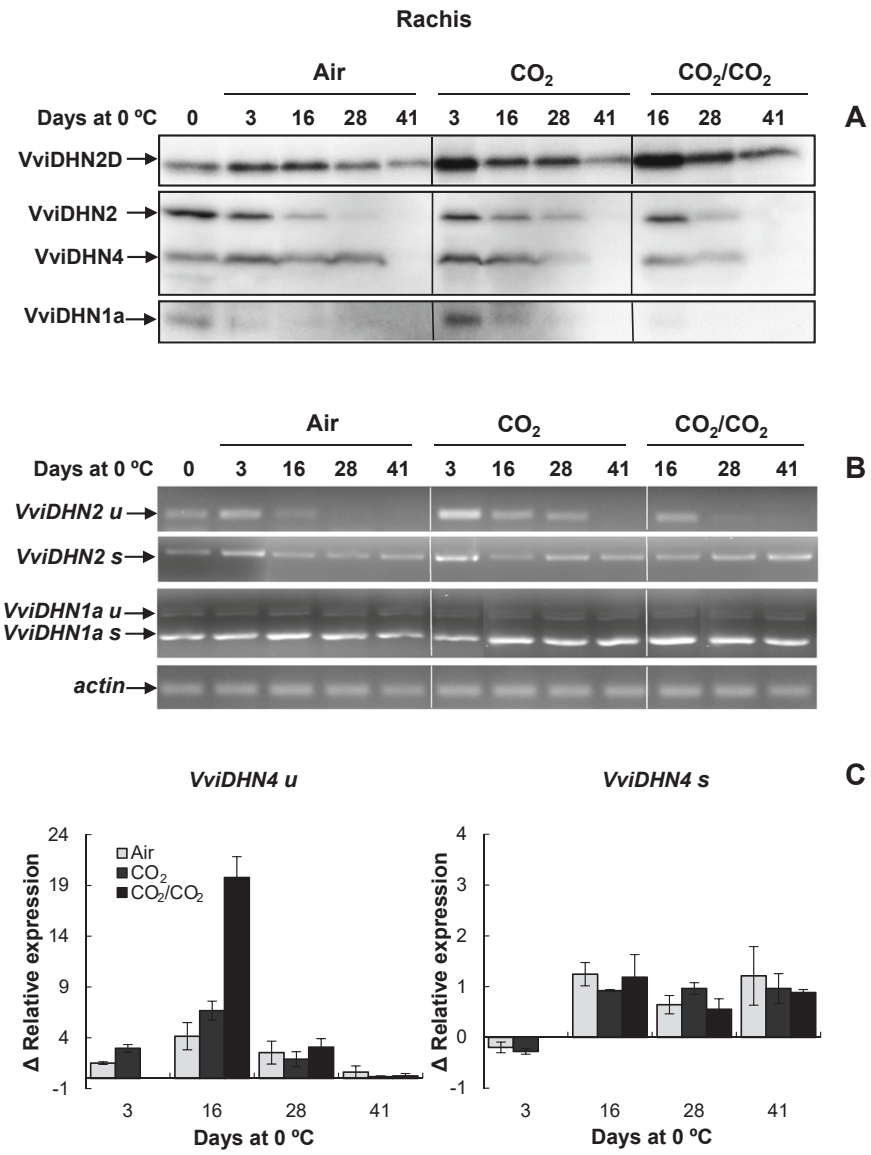

Fig. 5. Immunodetection of dehydrin isoforms (A) and levels of *VviDHN2*, *VviDHN1a* (B) and *VviDHN4* (C) spliced (s) and unspliced (u) mRNAs in the rachis of untreated (Air), CO_2-treated (CO_2) and CO_2/CO_2-treated (CO_2/CO_2) Autumn Royal table grapes during storage at 0 ºC. The results shown in A and B are representative of three biological samples. The relative expression of *VviDHN4* spliced and unspliced transcript levels was estimated using the $2^{-\Delta\Delta Ct}$ method, relative to the calibrator sample (prestored fruit, day 0). Data are the mean ± SD of three biological samples.

well as in the vacuole (Fig. 6B), chloroplast (Fig. 6B) and, to a lesser extent, in the cytoplasm (Fig. 6C) in prestored, along the cold storage period and in all pericarp tissue layers. Within the cell wall and the cytoplasm, PR-5 gold grains were detected scattered, without appearing as clusters or associated with osmiophilic elements contained therein, but in the vacuole, they were found both dispersed and forming small clusters (Fig. 6A and C). Within chloroplasts, thaumatin-like proteins were found specifically in areas of the lumen, with no immunolabeling associated with any of the organelle membranes (Fig. 6B). In this sense, no labelling was associated with any cell membrane, such as the plasma membrane, the nuclear membrane or the organelle membrane. Similarly, no hybridization of PR-5 antisera with mitochondria, nucleus or reticulum was observed (Fig. 6C and D).

At the subcellular level, dehydrins were detected mainly associated whit membranes, but were also found free in the cytoplasm, while no labelling was seen in the cell wall or vacuole (Fig. 7A and B). No change in the subcellular distribution was observed between prestored or untreated and treated pericarp tissue layers during the cold storage period (data not shown). In the plasmatic membranes, dehydrins were found in an arbitrary distribution, and did not form clusters at specific locations on the membrane (Fig. 7A and B). Dehydrins were also detected in the outer mitochondrial membrane, although its presence was more relevant inside the organelle, being located both in the matrix and associated with the membranes of the mitochondrial cristae (Fig. 7B). Particularly relevant was the intense labelling observed in chloroplasts, mainly associated with the lamellar and thylakoid membranes, although the image magnification allowed the visualization of gold particles in the stroma, not bound to membranes (Fig. 7C). Immunogold electron microscopy also localized the dehydrin proteins in the nucleus, where label was seen in both heterochromatin and euchromatin, associated with the nucleolus and nuclear membrane (Fig. 7D and E).

4. Discussion

Short-term high CO_2 treatment is a non-damaging and effective technology for delaying senescence-related changes and reducing dehydration and fungal decay without compromising table grape quality (Vazquez-Hernandez et al., 2018). More recently, we have shown that the application of a second short-term high CO_2 treatment significantly reduced the incidence and severity of long-term postharvest storage disorders (Vazquez-Hernandez et al., 2020). Furthermore, at the subcellular level, the study showed that CO_2 treatments restrain the ultrastructural damage associated with berry dehydration and oxidative stress. Like cell ultrastructure, pericarp microstructure analysis could

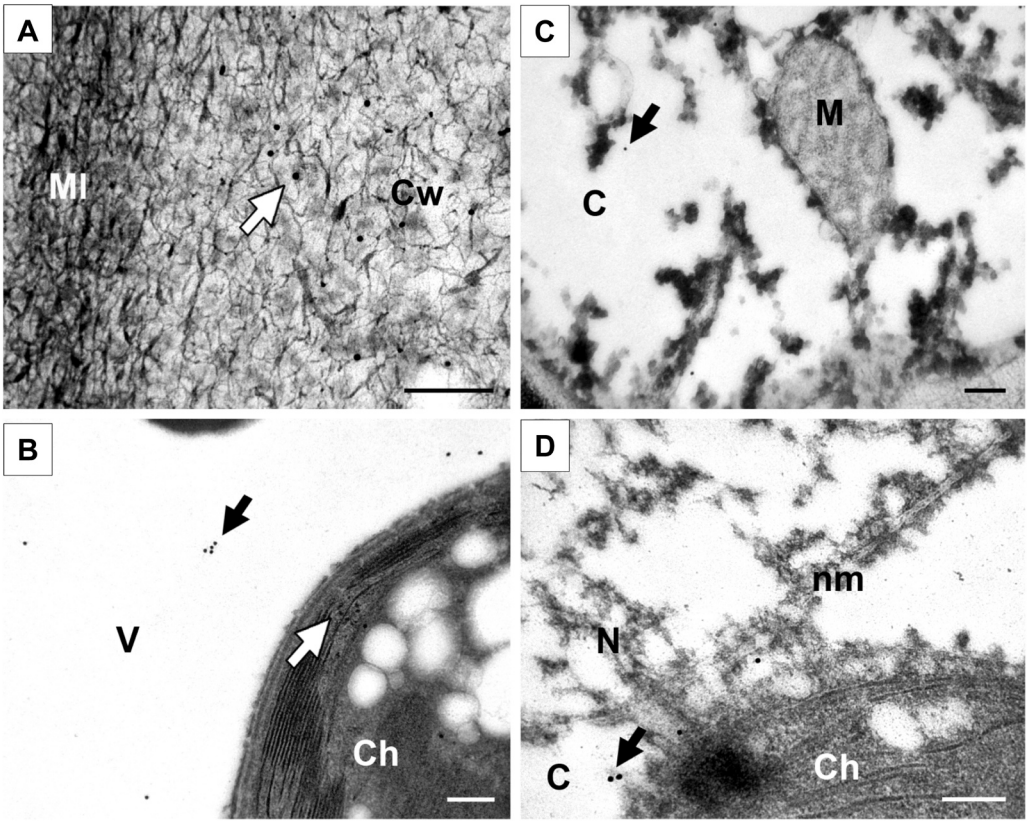

Fig. 6. Immunogold electron-microscope localization of thaumatin-like proteins in pericarp cells of Autumn Royal table grape. Representative images of subcellular localization from different cell compartments are shown. Cell wall (Cw), middle lamella (ML), cytoplasm (C), vacuole (V), chloroplast (Ch), mitochondria (M), nucleus (N), nuclear membrane (nm). Arrows indicate labelling of colloidal gold particles. Scale bars represent 0.2 μm. The micrographs shown are representative of six biological samples.

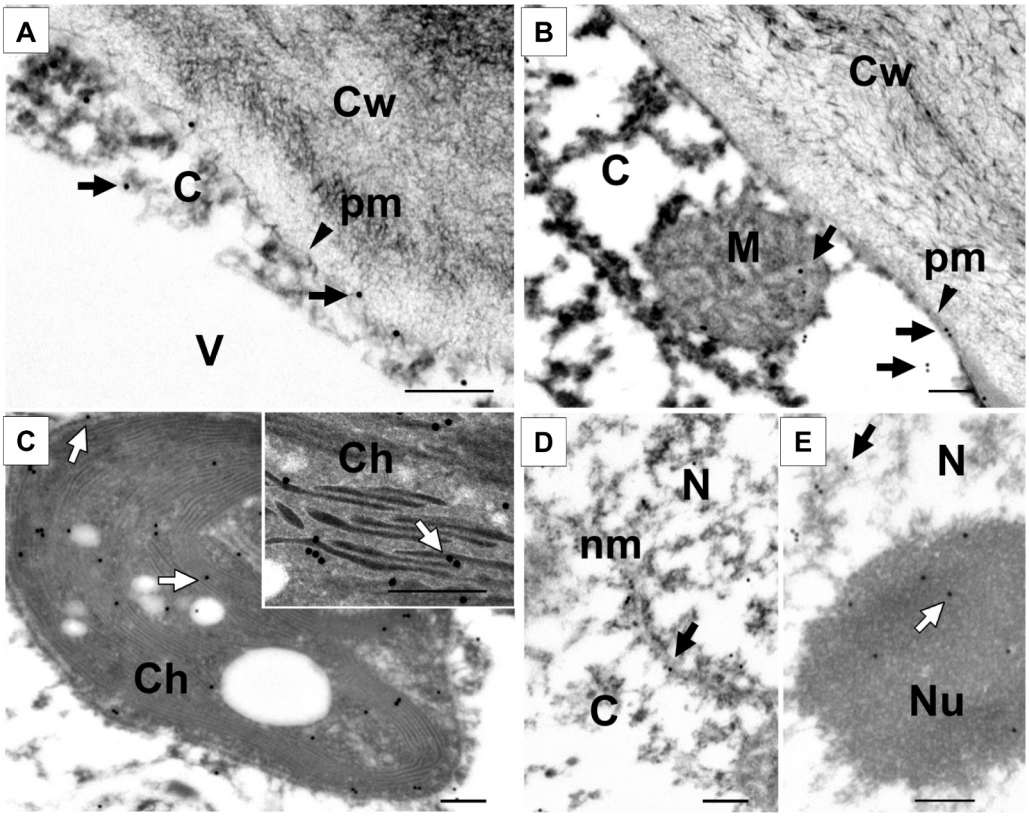

Fig. 7. Immunogold electron-microscope localization of dehydrins in pericarp cells of Autumn Royal table grape. Representative images of subcellular localization from different cell compartments are shown. Cell wall (Cw), plasma membrane (pm), cytoplasm (C), vacuole (V), chloroplast (Ch), mitochondria (M), nucleus (N), nuclear membrane (nm), nucleolus (Nu). Arrows indicate labelling of colloidal gold particles. Scale bars represent 0.2 μm. The micrographs shown are representative of six biological samples.

provide histological evidence for an overall assessment of the critical events associated with cold long-term postharvest disorders, as well as the tolerance response induced by CO_2 treatments. The analysis of the cell microstructure of Autumn Royal exocarp, unlike mesocarp, showed changes dependent on atmospheric storage conditions. Untreated fruit cells showed the highest degree of tissue disorganisation, which may be related to a loss of organization and compaction of the cell wall polymers, mainly pectin. These structural acidic heteropolysaccharides are associated with the primary cell wall and the middle lamella and are involved in the regulation of cell adhesion and the rigidity of tissues (Brummell, 2006). In addition to these features, and considering that pectic substances also determine the water holding capacity as well as the ion balance and ion transport in the cell wall, the observed structural modification could also be related to the loss of the hydration-homeostasis status of the berry cells. Unlike untreated berries, fruit treated with 20 kPa CO_2 for a short period of time retained a greater compaction of exocarp cells and a strengthening of the cell walls, probably due to the polymerization of pectic polysaccharides, which, due to their hydrophilic character and interaction with other cell wall polymers, structural proteins, polyamines, phenolic compounds and calcium ions, would contribute to the maintenance of the cell hydration level, cell structure and tissue morphology (Willats et al., 2001). At the microstructural level, the results also showed that the application of a second short-term high CO_2 treatment can improve the fruit's cell structure tolerance to long-term cold storage disorders.

In terms of cellular water loss and oxidative damage, we have established that several small organic molecules and dehydrins could be involved in the postharvest cold tolerance mechanism activated by the pretreatment with 20 kPa CO_2 for 3 d in the skin of Cardinal table grapes (Navarro et al., 2015; Vazquez-Hernandez et al., 2018). In this sense, it could be relevant for postharvest quality to know how the dual short-term high CO_2 treatment modulates the multifunctional stress responsible defence strategies, and whether they are tissue-dependent and time-regulated during long-term cold storage period in Autumn Royal table grape clusters. Since the metabolic response in terms of reactivity to external stimuli is different between grape berry tissues (Becatti et al., 2010), in this work we have analyzed the levels of different organic osmolytes, and their variation by the effect of postharvest environmental cues in skin and pulp separately. The results revealed a tissue-dependent endogenous environmental up-regulation of organic osmolytes which may be related to their active role in protecting against cold damage and dehydration. It has been widely described that trehalose, due to its physicochemical properties, plays an important cryoprotective role and has a high efficacy in the protection of membranes and biomolecules, replacing cellular water forming hydrogen bonds with membranes or by its ability to modify the solvation layer of the proteins during cold stress (John et al., 2017). The dose-dependent increase in skin trehalose biosynthesis could be functionally involved in the cryoprotective mechanism activated by high CO_2 levels, avoiding the enzyme and membrane structural damage caused by long-term storage at low temperatures under atmospheric conditions. This cold defense mechanism is more effective in the exocarp cells, which represent a fundamental protective barrier against damage caused by physical injury and pathogens.

Increased GABA accumulation in the skin could be related to its role in osmoregulation and protection against oxidative stress of cell membranes. In this sense, the tolerance of wheat cultivars to salt and osmotic stress has been shown to correlate with increased expression of glutamate decarboxylase and GABA accumulation (Al-Quraan et al., 2013). The idea that GABA has an antioxidant function is also supported by its subcellular, mitochondrial localization (Shelp et al., 2012). GABA treatment has also been shown to be an effective approach for maintaining postharvest quality and improving cold storage performance, due to a decrease in the content of reactive oxygen species and malondialdehyde, in parallel with an increase in the levels of antioxidant enzymes and maintenance of mitochondrial structure (Li et al., 2019). It is noteworthy that a dual treatment with 20 kPa CO_2 is the most effective in preserving chloroplast and mitochondrial membranes from long-term ultrastructural damage in exocarp and outer mesocarp tissues of Autumn Royal grapes (Vazquez-Hernandez et al., 2020). In addition, CO_2 treatments reduced cell and membrane oxidative damage and increased the unsaturation of 18-carbon fatty acid and lipid unsaturation ratio in the polar lipids of exocarp cell membranes (Vazquez-Hernandez et al., 2020).

Glycine betaine, in addition to being one of the most efficient osmoprotector in cells (Ashraf and Foolad, 2007; Lai et al., 2014), its effect on table grapes could also be related to membrane stabilization and detoxification of reactive oxygen species during cold storage (Awad et al., 2015). In this sense, there are researches suggesting that this quaternary amine enhances the degradation of H_2O_2 or maintains low level of $O_2^{\cdot}$ due to the enhancement of catalase and superoxide dismutase activity, respectively, thus stabilizing membrane integrity against extreme temperatures by reducing membrane lipid peroxidation, mainly in energetic organelles such as mitochondria and chloroplast (Chen et al., 2000; Park et al., 2007). Thus, the increased levels of glycine betaine, mainly in the pulp tissues, may help to protect the cellular machinery essential for repairing long-term cold-induced damage, as well as was previously proposed in chilling-sensitive fruit (Goñi et al., 2011). Likewise, a positive correlation between the accumulation of endogenous proline and improved cold and osmotic stress tolerance has been found mainly in chilling-sensitive fruit (Zhao et al. 2009). Given the location of this multifunctional non polar amino acid in the cytoplasm of stressed cells, where it plays the role of molecular chaperone and maintains the redox and energy status of the cell, it is important to note that the increase in proline levels is more significant in the pulp than in the skin tissues, where it could contribute more effectively to overcome the negative consequence of water deficit condition. In the active stress response of plants to changing environments, the role of proteins is crucial, as they are directly involved in the stress response both as structural proteins and also by regulating the plant epigenome, transcriptome and metabolome. Moreover, the function of proteins is not only dependent on their molecular structure, but also on their cellular localization, post-translational modifications and interacting partners (Kosová et al., 2018). Stress-related proteins whose constitutive levels increase in association with the tolerance response mechanism include protective functional protein families such as PRs and LEAs.

TLPs comprise unique proteins with diverse functions in host-pathogen interaction, stress tolerance and cell signaling (Liu et al., 2010). In table grape berries, two TLPs proteins, VvTL1 (a thaumatin-like protein encoded by the *VvTL1* gen) and VvTL2/VvTL3 (an osmotin-like protein encoded by the *VvTL2/VvTL3* gene; the so-called *VvOsm1* gene) are the most abundant PR proteins whose gene expression increases dramatically at the onset of sugar accumulation and berry softening (Loulakakis, 1997; Tattersall et al., 1997). Both *Vitis* TPLs exhibit potent antifungal activity *in vitro* and show a synergistic effect when present simultaneously (Monteiro et al., 2003). Consisting with the previous report on table grape (Tattersall et al., 1997), VviTL1 is constitutively expressed only in berry tissues, whereas VviOsmo protein was constitutively expressed, albeit at different levels, in berry tissues and rachis. It is worth noting the marked difference in the timing expression of the two TLPs in Autumn Royal cluster tissues. Whereas in rachis VviOsmo is downregulated and in skin tissues both TLPs are maintained at an initial state-stay level, in pulp tissues these defense protein isoforms are transcriptionally regulated differently by the duration of exposure to low temperature and atmospheric storage conditions. Moreover, whereas in pulp tissues the isoform expression and accumulation pattern of VviTL1 is mainly cold-regulated, that of VviOsmo was tightly regulated by CO_2, showing that the more short-term high CO_2 treatment is applied to Autumn Royal grapes, the more up-regulation of the VviOsmo isoform.

Thaumatin-like protein family has multiple roles to play in both biotic and abiotic stress tolerance. Despite their active fungal defense, the

members of this stress-responsive family could have other biological functions, such as the maintenance of cellular homeostasis or the stability of macromolecules and membranes, through their antifreeze or cryoprotective activity (Liu et al., 2010). Furthermore, the functional diversification of the members, even isoforms, of this conserved PR family could be related to their isoelectric point and cellular location. In general, extracellular TLPs tend to be acidic and contain an N-terminal signal peptide that targets mature proteins to the secretory pathway, whereas vacuolar TPLs, mainly osmotin and osmotin-like proteins, contain an additional C-terminal propeptide whose post-translational cleavage may be a requirement for vacuolar targeting (Anžlovar and Dermastia, 2003), as demonstrated by the vacuolar localization of tomato osmotins (Rodrigo et al., 1993). Therefore, to better understand the role of thaumatin-like proteins in postharvest table grapes, it is also necessary to determine their subcellular localization. Ultrastructural immunocytochemical localization revealed the presence of TLP isoforms in the cell wall, chloroplasts and vacuoles of Autumn Royal pericarp tissues. Based on the results of this work, the cold-responsive VviTL1 isoform could be associated with an extracellular antifungal and/or cryoprotective mechanism, as well as has been described by apoplastic leaf TLPs (Yu and Griffith, 1999) and various members of other PRs families in fruit (Goñi et al., 2010, 2011). On the other hand, the CO_2-responsive VviOsmo protein, probably located in the vacuole, in addition to its putative role in intracellular pathogen defence (Salzman et al., 1998), may be more related to the control of osmotic status. In this sense, the VviOsmo isoform could be more active in limiting osmotic and oxidative damage, maintaining the stability of proteins and cell membranes, resulting in increased cold dehydration tolerance. It has been reported that the expression of osmotin genes confers cell osmotic tolerance and antioxidant defense by facilitating the accumulation or compartmentalization of compatible and quenching reactive oxygen species and free radical solutes, as proline, or the expression of specific antioxidant enzymes, as superoxide dismutase or ascorbate peroxidase (Patade et al., 2013). In CO_2-treated mesocarp tissues, the increase in VviOsmo expression is concomitant accompanied by the highest accumulation of endogenous proline levels, which was also CO_2 dose-dependent. Moreover a link between the water stress tolerance mechanism, the enhancement of the amino acid metabolic flux to proline and GABA, and the improvement of the immune response in grapevine has been suggested (Hatmi et al., 2015). In this sense, the timing of accumulation of VviOsmo and VviTL1 in grape tissues correlated with naturally less decay, less cold-oxidative damage to cells and membranes, and also with less water loss in treated Autumn Royal berries (Vazquez-Hernandez et al., 2020). Recently, the transcriptional upregulation of the *VvOSM1* gene has been demonstrated in the response of grapevine to salt stress (Saleh and Alshehada, 2018). Furthermore, the subcellular localization of gold TLP grains in the thylakoid fraction could be related to the cryoprotective role of cell membrane integrity previously described by osmotin-like proteins, suggesting a functional role of these protective proteins in plant cold tolerance (Newton and Duman, 2000).

Dehydrins are another family of stress-responsive functional proteins. Transcriptomic analysis of the plant response to low temperature and drought stress revealed the induction of dehydrin gene expression (Tommasini et al., 2008). Similarly, it has been widely described that overexpression of dehydrins in transgenic plants may be sufficient to improve tolerance to drought, cold, and even freezing (Puhakainen et al., 2004, Bao et al., 2017). In *V. vinifera*, five genes encoding dehydrin-type proteins have been identified (Yang et al., 2012). *VviDHN1a*, *VviDHN2* and *VviDHN4* have been observed to have an alternative splicing consisting of the retention of an intron, resulting in truncated proteins (Fernandez-Caballero et al., 2012; Navarro et al., 2015). In previous work, we have shown that the application of a short-term high CO_2 treatment at the beginning of postharvest cold storage of cv. Cardinal induced the expression of spliced and unspliced *VviDHN1a* transcripts in the skin, pulp and seeds (Fernandez-Caballero et al., 2012), and spliced and unspliced forms of *VviDHN2* and *VviDHN4* in the skin (Navarro et al., 2015). Furthermore, the increased accumulation of VviDHN1a and VviDHN4 proteins, encoded by the *VviDHN1a* and *VviDHN4* genes, respectively, was mediated by the application of a 3 d 20 kPa CO_2 treatment in the skin of Cardinal table grapes stored at low temperature (Navarro et al., 2015). Recently, we have shown that the application of high CO_2 levels for 3 d at the beginning of cold storage, and in contrast to cv. Cardinal grapes, regulated mainly the intron retention in the *VviDHN* transcripts in Autumn Royal table grapes stored at 0 ºC in a cluster tissue different mode (Vazquez-Hernandez et al., 2017). In this work is shown that besides being expressed in a tissue-dependent manner, the dual short-term high CO_2 treatment carries out a differential regulation of *VviDHN* expression, activating mainly the unspliced forms of *VvDHN4*. This post-transcriptional regulatory mechanism could be part of the biotic defence mechanism activated by high CO_2 levels (Rosales et al., 2014).

On the other hand, the particular behavior of the dehydrin spliced forms highlights the sharp difference between cluster tissues in terms of reactivity to external stimuli. This work shows for the first time the postharvest accumulation pattern of this multifamily protein in the rachis and shows that they are not directly involved in the beneficial effect of high CO_2, which reduces cluster weight loss and rachis browning during postharvest storage (Vazquez-Hernandez et al., 2017; Vazquez-Hernandez et al., 2020). On the other hand, in berry tissues, the pattern of expression and accumulation of VviDHN isoforms depends on tissue and atmospheric composition. While the dimeric and monomeric VviDHN2 isoforms are cold-regulated in pulp tissues, only VviDHN2D is up-regulated in the skin. On the other hand, VviDHN2, VviDHN4 and VviDHN1a are CO_2 transcriptionally regulated in both grape tissues. It should be noted that in pulp tissues, where very low levels of constitutive monomeric isoforms were detected in prestored fruit, VviDHN4 and VviDHN1a were the isoforms that are mainly up-regulated by the dual short-term high CO_2 treatment. It is worth noting that VviDHN1a and VviDHN4, both Y_nSK_n type dehydrins, could be functionally concerned in the active defense-related response associated with dual CO_2 treatment by efficiently acting as a molecular shield to protect proteins and cellular membranes from freezing and mainly from dehydration, with VviDHN4 exhibiting a great potential as reactive oxygen species scavenger (Vazquez-Hernandez et al., 2021). In addition to the diversification of protein function-interaction, dehydrins could be associated with specific subcellular structures. Immunocytochemical localization of all spliced *V. vinifera* dehydrins (without differentiation by isoforms) showed a strong labelling in the cell membranes of Autumn Royal pericarp. It has been suggested that the ability of dehydrins to lower the temperature of the lipid transition phase lies in their capacity to bind to the periphery of the membranes, probably inserting the K- lysine side chains, as well as in their capacity to ensure the availability of water molecules destined for the hydration of the polar heads of phospholipids, due to their high hydrophilicity (Clarke et al., 2015). In addition, conserved sequences of dehydrins have a α-helical amphipathic domain with both water binding and hydrophobic interaction potential. The accumulation of an acidic dehydrin in the vicinity of the plasma membrane has been described during low temperature acclimation of wheat (Danyluk et al., 1998), as well as the constitutive presence of this protein family in mitochondria of wheat, rye and maize seeds (Borovskii et al., 2002). In this sense, our results indicated that the outer membrane of mitochondria also showed colloidal gold labelling, although the presence of dehydrins was more relevant inside the organelle, both in the matrix and in the mitochondrial crests membranes. Particularly relevant was the intense labelling found associated with the chloroplast lamellar, outer membrane and thylakoid membranes. Previously, similar results had been observed in leaf tissues of *Pissum sativum* and *Zea mays* following chloroplast fractionation tests and visualization by immunomicroscopy (Mueller et al., 2003). The nucleus was another organelle that showed a high level of immunolabeling, with the dehydrins located in the nuclear double membrane, in the interior of the nucleus,

associated or unassociated with chromatin, and in the nucleolus. Previous studies have attributed the ion-binding activity and the nuclear location of the dehydrins to phosphorylation of the S segment and the adjacent Ser and Tyr residues by protein kinases (Alsheikh et al., 2003). In addition, it has been suggested that some atypical segments, such as the fixed motif GX(Q)GGRRKK that link the K- and S-segments and that is present in many Y_nSK_n type dehydrins, as VviDHN1a and VviDHN4 (Vazquez-Hernandez et al., 2021), participates on the one hand in the interaction of negatively-charged phosphoserines with the K-segment, GXGG motif, and on the other hand as a nuclear localization signal, RRKK motif (Yu et al., 2018). Likewise, the analysis of the location of the dehydrin allowed to observer their distribution in the cellular cytoplasm, which did not respond to any type of cellular polarization, being randomly and homogeneously located throughout the cytoplasmic space. Finally, contrary to the observations of Puhakainen et al. (2004), no presence of gold labeling was detected in other organelles such as the vacuole, neither in the endoplasmic reticulum nor in the cell wall.

In conclusion, the efficacy of the application of a dual short-term CO_2 treatment in delaying the decline in harvested cluster quality caused by senescence and long-term postharvest cold-storage disorders is associated with differential timing and tissue-dependent transcriptional regulation of stress-responsive TLP and VviDHN isoforms, based on their differences in cellular location and biological function, as well as the redirection of metabolism towards the synthesis of active osmoprotective solutes. Among these multifunctional biomolecules, CO_2 treatment in skin tissues regulates the expression of the VviDHN isoforms, mainly the unspliced forms, and activates the trehalose synthesis, both functionally involved in the cell and membrane cryoprotective mechanism of cold tolerance activated by CO_2. On the other hand, in mesocarp tissues, the active prevailing defense response related to CO_2 treatments, in a closely dose dependent manner, was the up-regulation of those more effective strategies involved in the cell osmotic adjustment and oxidative damage, as VviOsmo, VviDHN4, VviDHN1a and proline, preventing the dehydration disorders caused by senescence and cold postharvest storage. The results also showed that the more short-term high CO_2 treatment is applied to Autumn Royal grapes, the more cell microstructural evidence there is of enhanced tolerance to long-term cold and prevention of storage disorders in terms of thicker and denser cell wall that could contribute to restrain swelling, dehydration and osmotic stress.

CRediT authorship contribution statement

Conceptualization, M.I.E.; Formal analysis and Investigation, all authors; Methodology, M.V-H, I.R.; Project administration, M.I.E; Supervision and Coordination the experiments, M.I.E: Writing – original draft preparation, M.I.E. Writing – review & editing, all authors.

All authors have read and agreed to the published version of the manuscript.

Declaration of Competing Interest

The authors declare the following financial interests/personal relationships which may be considered as potential competing interests: Maria Isabel Escribano reports financial support was provided by Spanish Ministry of Science and Innovation. Maria Teresa Sanchez-Ballesta reports financial support was provided by Spanish Ministry of Science and Innovation.

Data Availability

Data will be made available on request.

Acknowledgements

The authors thank M.L. García of the National Centre for Electron Microscopy, Faculty of Chemistry, Complutense University of Madrid, for technical assistance with the Transmission Electron Microscopy analysis and to M. Legrand (Strasbourg, France) for his generosity in providing PR-5 antisera. This research was supported by the Spanish CICYT projects AGL2017-85291-R (MINECO/AEI/FEDER, UE) and PID2020–113965RB-I00/AEI/10.13039/501100011033. M. Vazquez-Hernandez acknowledges the support of the FPI programme financed by the MICINN.

References

Al-Quraan, N.A., Sartawe, F.A., Qaryout, M.M., 2013. Characterization of gamma-aminobutyric acid metabolism and oxidative damage in wheat (*Triticum aestivum* L.) seedlings under salt and osmotic stress. J. Plant Physiol. 170, 1003–1009.

Alsheikh, M.K., Heyen, B.J., Randall, S.K., 2003. Ion binding properties of the dehydrin ERD14 are dependent upon phosphorylation. J. Biol. Chem. 278, 40882–40889.

Anžlovar, S., Dermastia, M., 2003. The comparative analysis of osmotins and osmotin-like PR-5 proteins. Plant Biol. 5, 116–124.

Ashraf, M., Foolad, M.R., 2007. Roles of glycine betaine and proline in improving plant abiotic stress resistance. Environ. Exp. Bot. 59, 206–216.

Awad, M.A., Al-Qurashi, A.D., Mohamed, S.A., 2015. Postharvest *trans*-resveratrol and glycine betaine treatments affect quality, antioxidant capacity, antioxidant compounds and enzymes activities of 'El-Bayadi' table grapes after storage and shelf life. Sci. Hortic. 197, 350–356.

Bao, F., Du, D., An, Y., Yang, W., Wang, J., Cheng, T., Zhang, Q., 2017. Overexpression of *Prunus mume* dehydrin genes in tobacco enhances tolerance to cold and drought. Front. Plant Sci. 8, 151.

Becatti, E., Chkaiban, L., Tonutti, P., Forcato, C., Bonghi, C., Ranieri, A.M., 2010. Short-term postharvest carbon dioxide treatments induce selective molecular and metabolic changes in grape berries. J. Agric. Food Chem. 58, 8012–8020.

Blanch, M., Fernandez-Caballero, C., Sanchez-Ballesta, M.T., Escribano, M.I., Merodio, C., 2014. Accumulation and distribution of potassium and its association with water balance in the skin of Cardinal table grapes during storage. Sci. Hortic. 175, 223–228.

Borovskii, G.B., Stupnikova, I.V., Antipina, A.I., Vladimirova, S.V., Voinikov, V.K., 2002. Accumulation of dehydrin-like proteins in the mitochondria of cereals in response to cold, freezing, drought and ABA treatment. BMC Plant Biol. 2, e5.

Brummell, D.A., 2006. Cell wall disassembly in ripening fruit. Funct. Plant Biol. 33, 103–119.

Chen, W., Li, P., Chen, T., 2000. Glycine betaine increases chilling tolerance and reduces chilling-induced lipid peroxidation in *Zea mays* L. Plant Cell Environ. 23, 609–618.

Chen, J.Y., Wen, P.F., Kong, W.F., Pan, Q.H., Wan, S.B., Huang, W.D., 2006. Changes and subcellular localizations of the enzymes that involved in pheylpropanoid metabolism during grape berry development. J. Plant Physiol. 163, 115–127.

Clarke, M.W., Boddington, K.F., Warnica, J.M., Atkinson, J., Mckenna, S., Madge, J., Barker, C.H., Graether, S.P., 2015. Structural and functional insights into the cryoprotection of membranes by the intrinsically disordered dehydrins. J. Biol. Chem. 290, 26900–26913.

Danyluk, J., Perron, A., Houde, M., Limin, A., Fowler, B., Benhamou, N., Sarhan, F., 1998. Accumulation of an acidic dehydrin in the vicinity of the plasma membrane during cold acclimation of wheat. Plant Cell 10, 623–638.

Fernandez-Caballero, C., Rosales, R., Romero, I., Escribano, M.I., Merodio, C., Sanchez-Ballesta, M.T., 2012. Unraveling the roles of *CBF1*, *CBF4* and dehydrin 1 genes in the response of table grapes to high CO_2 levels and low temperature. J. Plant Physiol. 169, 744–748.

Goñi, O., Sanchez-Ballesta, M.T., Merodio, C., Escribano, M.I., 2010. Potent cryoprotective activity of cold and CO_2-regulated cherimoya (*Annona cherimola*) endochitinase. J. Plant Physiol. 167, 1119–1129.

Goñi, O., Sanchez-Ballesta, M.T., Merodio, C., Escribano, M.I., 2011. A cryoprotective and cold-adapted 1,3-β-endoglucanase from cherimoya (*Annona cherimola*) fruit. Phytochemistry 72, 844–854.

Griffith, M., Yaish, M.W.F., 2004. Antifreeze proteins in overwintering plants: a tale of two activities. Trends Plant Sci. 9, 399–405.

Hatmi, S., Gruau, C., Trotel-Aziz, P., Villaume, S., Rabenoelina, F., Baillieul, F., Eullaffroy, P., Clément, C., Ferchichi, A., Aziz, A., 2015. Drought stress tolerance in grapevine involves activation of polyamine oxidation contributing to improved immune response and low susceptibility to *Botrytis cinerea*. J. Exp. Bot. 66, 775–787.

John, R., Raja, V., Ahmad, M., Jan, N., Majeed, U., Ahmad, S., Yaqoob, U., Kaul, T., 2017. Trehalose: metabolism and role in stress signaling in plants. In: Sarwat, M., Ahmad, A., Abdin, M.Z., Ibrahim, M.M. (Eds.), Stress Signaling in Plants: Genomics and Proteomics Perspective, Vol. 2. Springer International Publishing, Switzerland, pp. 261–275.

Kosová, K., Vítámvás, P., Prášil, I.T., Renaut, J., 2011. Plant proteome changes under abiotic stress. Contribution of proteomics studies to understanding plant stress response. J. Proteomics 1301–1322.

Kosová, K., Vítámvás, P., Urban, M.O., Prášil, I.T., Renaut, J., 2018. Plant abiotic stress proteomics: The major factors determining alterations in cellular proteome. Front. Plant Sci. 9, 122.

Lai, S.J., Lai, M.C., Lee, R.J., Chen, Y.H., Yen, H.E., 2014. Transgenic Arabidopsis expressing osmolyte glycine betaine synthesizing enzymes from halophilic methanogen promote tolerance to drought and salt stress. Plant Mol. Biol. 85, 429–441.

Li, J., Zhou, X., Wei, B., Cheng, S., Zhou, Q., Ji, S., 2019. GABA application improves the mitochondrial antioxidant system and reduces peel browning in "Nanguo" pears after removal from cold storage. Food Chem. 297, 124903.
Liu, J.J., Sturrock, R., Ekramoddoullah, A., 2010. The superfamily of thaumatin-like proteins: its origin, evolution, and expression towards biological function. Plant Cell. Rep. 29, 419–436.
Loulakakis, K.A., 1997. Genomic organisation and expression of an osmotin-like gene in *Vitis vinifera* L. Vitis 36, 57–158.
Monteiro, S., Barakat, M., Piçarra-Pereira, M.A., Teixeira, A.R., Ferreira, R.B., 2003. Osmotin and thaumatin from grape: A putative general defense mechanism against pathogenic fungi. Phytopathology 93, 1505–1512.
Mueller, J.K., Heckathorn, S.A., Fernando, D., 2003. Identification of a chloroplast dehydrin in leaves of mature plants. Inter. J. Plant Sci. 164, 535–542.
Navarro, S., Vazquez-Hernandez, M., Rosales, R., Sanchez-Ballesta, M.T., Merodio, C., Escribano, M.I., 2015. Differential regulation of dehydrin expression and trehalose levels in Cardinal table grapes skin by low temperature and high CO_2. J. Plant Physiol. 179, 1–11.
Newton, S.S., Duman, J.G., 2000. An osmotin-like cryoprotective protein from the bittersweet nightshade *Solanum dulcamara*. Plant Mol. Biol. 44, 581–589.
Park, E.J., Jeknić, Z., Pino, M.T., Murata, N., Chen, T.H.H., 2007. Glycine betaine accumulation is more effective in chloroplasts than in the cytosol for protecting transgenic tomato plants against abiotic stress. Plant Cell Environ. 30, 994–1005.
Patade, V.Y., Khatri, D., Kumari, M., Grover, A., Gupta, S.M., Ahmed, Z., 2013. Cold tolerance in osmotin transgenic tomato (*Solanum lycopersicum* L.) is associated with modulation in transcript abundance of stress responsive genes. SpringerPlus 2, 117.
Puhakainen, T., Hess, M.W., Makela, P., Svensson, J., Heino, P., Palva, E.T., 2004. Overexpression of multiple dehydrin genes enhances tolerance to freezing stress in *Arabidopsis*. Plant Mol. Biol. 54, 743–753.
Rodrigo, I., Vera, P., Tornero, P., Hernandez-Yago, J., Conejero, V., 1993. cDNA cloning of viroid-induced tomato pathogenesis-related protein P23. Characterization as a vacuolar antifungal factor. Plant Physiol. 102, 939–945.
Romero, I., Vázquez-Hernández, M., Escribano, M.I., Merodio, C., Sanchez-Ballesta, M.T., 2016. Expression profiles and DNA-binding affinity of five ERF genes in bunches of *Vitis vinifera* cv. Cardinal treated with high levels of CO_2 at low temperature. Front. Plant Sci. 7, 1748.
Romero, I., Vazquez-Hernandez, M., Tornel, M., Escribano, M.I., Merodio, C., Sanchez-Ballesta, M.T., 2021. The effect of ethanol treatment on the quality of a new table grape cultivar It 681-30 stored at low temperature and after a 7-day shelf-life period at 20 °C: A molecular approach. Int. J. Mol. Sci. 22, 8138.
Rosales, R., Fernandez-Caballero, C., Romero, I., Escribano, M.I., Merodio, C., Sanchez-Ballesta, M.T., 2013. Molecular analysis of the improvement in rachis quality by high CO_2 levels in table grapes stored at low temperature. Postharvest Biol. Technol. 77, 50–58.
Rosales, R., Romero, I., Escribano, M.I., Merodio, C., Sanchez-Ballesta, M.T., 2014. The crucial role of Φ-and K-segments in the in vitro functionality of *Vitis vinifera* dehydrin DHN1a. Phytochemistry 108, 17–25.
Saleh, B., Alshehada, E., 2018. Transcriptional analysis of *VvOSM1* gene in grapevine (*Vitis vinifera* L.) under salt stress. J. Plant Biochem. Physiol. 6, 1000217.
Salzman, R.A., Tikhonova, I., Bordelon, B.P., Hasegawa, P.M., Bressan, R.A., 1998. Coordinate accumulation of antifungal proteins and hexoses constitutes a developmentally controlled defense response during fruit ripening in grape. Plant Physiol. 117, 465–472.
Sevillano, L., Sanchez-Ballesta, M.T., Romojaro, F., Flores, F.B., 2009. Physiological, hormonal and molecular mechanisms regulating chilling injury in horticultural species. Postharvest technologies applied to reduce its impact. J. Sci. Food Agric. 89, 555–573.
Sharma, P., Jha, B.A., Dubey, R.S., Pessarakli, M., 2012. Reactive oxygen species, oxidative damage, and antioxidative defense mechanism in plants under stressful conditions. J. Bot. Artic., 217037, 26 pages.
Shelp, B.J., Bozzo, G.G., Trobacher, C.P., Chiu, G., Bajwa, V.S., 2012. Strategies and tools for studying the metabolism and function of γ-aminobutyrate in plants. I. Pathway structure. Botany 90, 781–793.
Tattersall, D.B., van Heeswijck, R., Høj, P.B., 1997. Identification and characterization of a fruit-specific, thaumatin-like protein that accumulates at very high level in conjunction with the onset of sugar accumulation and berry softening in grapes. Plant Physiol. 114, 759–769.
Tian, S., Qin, G., Li, B., 2013. Reactive oxygen species involved in regulating fruit senescence and fungal pathogenicity. Plant Mol. Biol. 82, 593–602.
Tommasini, L., Svensson, J.T., Rodriguez, E.M., Wahid, A., Malatrasi, M., Kato, K., Wanamaker, S., Resnik, J., Close, T.J., 2008. Dehydrin gene expression provides an indicator of low temperature and drought stress: transcriptome-based analysis of barley (*Hordeum vulgare* L.). Func. Integr. Genom. 8, 387–405.
Vazquez-Hernandez, M., Blanch, M., Sanchez-Ballesta, M.T., Merodio, C., Escribano, M. I., 2020. High CO_2 alleviates cell ultrastructure damage in Autumn Royal table grapes by modulating fatty acid composition and membrane and cell oxidative status during long-term cold storage. Postharvest Biol. Technol. 160, 111037.
Vazquez-Hernandez, M., Navarro, S., Sanchez-Ballesta, M.T., Merodio, C., Escribano, M. I., 2018. Short-term high CO_2 treatment reduces water loss and decay by modulating defense proteins and organic osmolytes in Cardinal table grape after cold storage and shelf-life. Sci. Hortic. 234, 27–35.
Vazquez-Hernandez, M., Romero, I., Escribano, M.I., Merodio, C., Sanchez-Ballesta, M.T., 2017. Deciphering the role of CBF/DREB transcription factors and dehydrins in maintaining the quality of table grapes cv. Autumn Royal treated with high CO_2 levels and stored at 0°C. Front. Plant Sci. 8, 1591.
Vazquez-Hernandez, M., Romero, I., Sanchez-Ballesta, M.T., Merodio, C., Escribano, M.I., 2021. Functional characterization of VviDHN2 and VviDHN4 dehydrin isoforms from *Vitis vinifera* (L.): An *in silico* and *in vitro* approach. Plant Physiol. Biochem 158, 146–157.
Willats, W.G.T., McCartney, L., Mackie, W., Knox, J.P., 2001. Pectin: cell biology and prospects for functional analysis. Plant Mol. Biol. 47, 9–27.
Yang, Y., He, M., Zhu, Z., Li, S., Xu, Y., Zhang, C., Singer, S.D., Wang, Y., 2012. Identification of the *dehydrin* gene family from grapevine species and analysis of their responsiveness to various forms of abiotic and biotic stress. BMC Plant Biol. 12, e140.
Yu, X.M., Griffith, M., 1999. Antifreeze proteins in winter rye leaves form oligomeric complexes. Plant Physiol. 119, 1361–1369.
Yu, Z., Wang, X., Zhang, L., 2018. Structural and functional dynamics of dehydrins: a plant protector protein under abiotic stress. Int. J. Mol. Sci. 19, 3420.
Zhao, D.Y., Shen, L., Fan, B., Liu, K.L., Yu, M.M., Zheng, Y., Ding, Y., Sheng, J.P., 2009. Physiological and genetic properties of tomato fruit from 2 cultivars differing in chilling tolerance at cold storage. J. Food Sci. 74, 348–352.